

# Reliability based multidisciplinary design optimization of cooling turbine blade considering uncertainty data statistics

Lei Li<sup>1</sup> · Huan Wan<sup>1</sup> · Wenjing Gao<sup>1</sup> · Fujuan Tong<sup>1</sup> · Honglin Li<sup>1</sup>

Received: 7 February 2018 / Revised: 15 August 2018 / Accepted: 26 August 2018 / Published online: 19 September 2018  
© Springer-Verlag GmbH Germany, part of Springer Nature 2018

## Abstract

Considering the coupling among aerodynamic, heat transfer and strength, a reliability based multidisciplinary design optimization method for cooling turbine blade is introduced. Multidisciplinary analysis of cooling turbine blade is carried out by sequential conjugated heat transfer analysis and strength analysis with temperature and pressure interpolation. Uncertainty data including the blade wall, rib thickness, elasticity Modulus and rotation speed is collected. Data statistics display the probability models of uncertainty data follow three-parameter Weibull distribution. The thickness of blade wall, thickness and height of ribs are chosen as design variables. Kriging surrogate model is introduced to reduce time-consuming multidisciplinary reliability analysis in RBMDO loop. The reliability based multidisciplinary design optimization of a cooling turbine blade is carried out. Optimization results shows that the RBMDO method proposed in this work improves the performance of cooling turbine blade availably.

**Keywords** Cooling turbine blade · Reliability based multidisciplinary design optimization · Kriging surrogate model · Uncertainty data statistics

## 1 Introduction

Due to the increasing turbine inlet temperature, the high-pressure turbine blade must be cooled so as to work at a suitable temperature. Generally, the cooling turbine blade that is hollow inside is made by a complex casting technology. Such casting process will unavoidably cause the dispersion of material properties and wall thickness. These dispersions together with the uncertainties of working temperature, rotation speed and so on could have a serious effect on the serving life of turbine blades. Especially, the modern gas turbine is designed by optimization method and the design result is at the boundary between feasible domain and infeasible domain. A small disturbance caused by uncertainties could lead the optimized results to fall into an infeasible domain and will significantly affect its safety (Saad et al. 2016). Therefore, it is crucial to

take into account the uncertain factors when designing the modern cooling turbine blade.

Design of cooling turbine blade is a typical multidisciplinary design optimization (MDO) problem, which involves several coupled disciplines such as aerodynamic, heat transfer and strength. The uncertainties will spread among the coupling disciplines, making the reliability analysis and design of multidisciplinary systems to be more complex. Firstly, the deterministic MDO methods without considering the uncertainties are developed. Perez et al. (2004) introduced the Multidisciplinary Feasible Design (MDF) method which was a single-level MDO framework and consisted of a multidisciplinary analysis (MDA) module and an optimization module. In the MDA module, the multiple disciplines were analyzed in turn under the coupling information transfer to implement coupling analysis. The MDA module was carried out in the optimization module to obtain the optimal solution. In order to avoid the sequence analysis of multiple disciplines which will spend a lot of computing time, Park et al. (2002) proposed the Individual Discipline Feasible (IDF) method. In the IDF method, the multiple disciplines of MDO system can be analyzed in parallel, in which the coupling variables were proposed and satisfied the consistency constraints to complete coupling analysis. Furthermore, considering the optimal solution of the MDO system should be closely related to the optimal

---

Responsible Editor: Mehmet Polat Saka

---

✉ Lei Li  
lileinpu@nwpu.edu.cn

<sup>1</sup> Department of Engineering Mechanics, Northwestern Polytechnical University, Xi'an 710072, Shaanxi, China

solution of each discipline, so the global optimal solution of MDO system could be more easily obtained on basis of the optimal solution of each discipline. Therefore, the two-level MDO framework consisting of discipline level optimization and system level optimization was developed. Collaborative Optimization (CO) (Wang et al. 2013), Concurrent Subspace Optimization (CSSO) (Sellar et al. 1996) and Bi-Level Integrated System Synthesis method (BLISS) (Zhou et al. 2014) are the typical two-level optimization systems. Currently, the developed MDO method and its idea has become an essential tool for complex system design, which is widely applied in the design of aerospace, aircrafts (Deng and Suresh 2017a, b), vehicles, propulsion systems (Deng and Suresh 2017a, b), energy and other industries.

On basis of the deterministic MDO methods, a series of reliability-based multidisciplinary design optimization (RBMDO) methods have been developed. Nikbay and Kuru (2013) introduced the structural and aerodynamic uncertainties into MDF framework and proposed a RBMDO-MDF method for aircraft wing. The loosely coupled aeroelastic analysis (multidisciplinary analysis) was solved by finite volume-based flow solver, finite element solver, pressure and displacement information exchanging. On basis of aeroelastic analysis, a first-order reliability analysis method was used to evaluate the probability of failure. This RBMDO-MDF framework composed of multidisciplinary analysis, reliability analysis and optimization is a tri-nested loop. In order to improve the optimization efficiency of the RBMDO-MDF with tri-nested loop, Hui and Weiji (2008) combined CSSO method and the advanced first order second moment reliability analysis method to develop a RBMDO-CSSO method. The deterministic optimization by CSSO was carried out to obtain the initial design for RBDO. Then, the optimal design was founded by using the polynomial based RSM. In this method, the reliability analysis was decoupled from the optimization process to improve the efficiency of optimization. Huang et al. (2018) proposed a decoupling algorithm of RBMDO which decoupled the MDO system by IDF to convert the RBMDO to a conventional RBDO and used incremental shifting vector strategy to optimization and reliability analysis to enhance the efficiency and convergence of the overall solving process. Ahn and Kwon (2006) proposed a RBMDO method based on BLISS in which the reliability analysis and optimization were conducted in a sequential manner by approximating limit state functions. Du et al. (2008) introduced a sequential optimization and reliability assessment (SORA) method which decoupled a RBMDO problem into a sequential of deterministic MDO and reliability analysis. Yao et al. (2011) presented the review of reliability-based multidisciplinary design optimization method and the state of the art in RBMDO methods for aerospace vehicles. The proposed methods that have been proved to be highly efficient and applied in MDO systems can provide support for the reliability based multidisciplinary design optimization of cooling turbine blade.

For a complex MDO system, its responses usually cannot be predicted by explicit functions and should be simulated with the help of commercial software which may take a lot of computing time. In order to reduce the computing time of discipline analysis, surrogate model which fits the output responses with input parameters of disciplines are developed to replace the large-scale simulation computation in the RBMDO loop. Meng et al. (2015) employed the response surface model in the RBMDO-SORA of a hydraulic transmission mechanism to reduce its coupled analysis time. Roshanian and Ebrahimi (2013) also employed response surface model to obtain propulsion, weight, aerodynamics and trajectory of a two-stage solid propellant expendable launch vehicle and carried out the RBMDO of the launch vehicle. Besides, Chen et al. (2014) and Li et al. (2016) adopted the Kriging surrogate model into RBMDO method to improve optimization efficiency. The above researches which have proved that using surrogate model in RBMDO can improve the optimization efficiency significantly can also provide support for the RBMDO of cooling turbine blade.

Currently, the RBMDO method and surrogate model have been applied in the aircraft, launch vehicle and other products. Because that the uncertainties and the coupling characteristic of cooling turbine blade are different from the aircraft and launch vehicle, the current method should be further developed for the RBMDO of cooling turbine blade. On the reliability design of turbine blade, Fei and Bai (2012) assumed that the random variables which included rotor speed, gas temperature and heat transfer parameters obeyed the normal distribution and analyzed the reliability of a turbine blade which only considered nonlinear dynamic. Wong et al. (2013) used the Fourier series method to compute the linear fuzzy reliability of Normal distributed stress or strength. Gao et al. (2016) analyzed the low-cycle fatigue reliability of a turbine blade with the help of distributed collaborative response surface. Song et al. (2017a, b) assumed that the random variables which included inlet velocity, inlet pressure, gas temperature, material density and rotor speed obeyed normal distribution and carried out a multi-objective reliability based design optimization of a turbine blisk using artificial neural network. In the above works of turbine blade reliability, that random variables are usually assumed to obey the normal distribution does not meet the actual situation. The turbine blades analyzed above are all solid blade and do not consider the cooling structure features. Meanwhile, the above works for turbine blade reliability are basically about a single discipline, do not consider the coupling of multiple disciplines in the design of turbine blade.

In this work, the data for main random variables which are wall thickness, material mechanical properties of cooling turbine blade are counted and the RBMDO method considering the structure and coupling features of cooling turbine blades is developed. The paper is organized as follows. In section 2, the RBMDO method for cooling turbine blades is introduced. The

multidisciplinary analysis of a cooling turbine blade is performed in section 3. In section 4, probability distributions of random variables are presented. Finally, RBMDO of the cooling turbine blade is carried out and discussed.

## 2 RBMDO method for cooling turbine blade

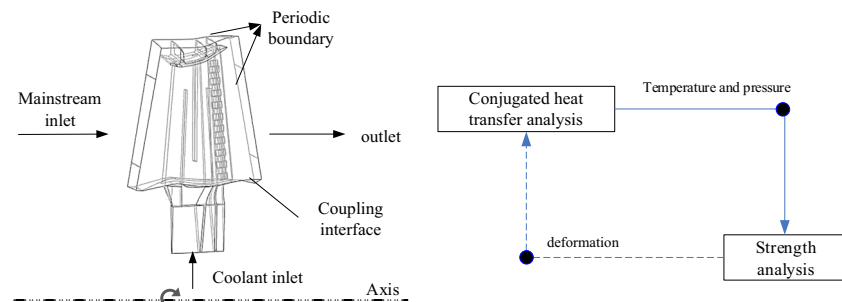
Cooling turbine blade that works in a high temperature, pressure and rotation speed condition suffers strong fluid-thermal-solid interaction. Figure 1 demonstrates the structure of a cooling turbine blade and the coupling relationship between cooling disciplines involved in its design. Due to the complex fluid-structure coupling interface, conjugated heat transfer method that takes into account both heat conduction in solid domain and heat flow in fluid domain is employed to simulate convective heat transfer analysis of the cooling turbine blade. However, the conjugated heat transfer analysis needs a long time to converge (Bejan 2013), and together with structural analysis and the interactions between them, computing cost for the coupled fluid-thermal-solid analysis can be extremely huge.

On basis of fluid-thermal-solid interaction and considering random variables, cooling turbine blade reliability analysis with multidisciplinary coupling can be carried out. Because that the time-consuming fluid-thermal-solid interaction analysis needs to be repeated for many times in the reliability analysis and reliability-based optimization design, the reduction of computing time become crucial for RBMDO. Therefore, surrogate model is introduced to replace the fluid-thermal-solid interaction analysis and Fig. 2 gives the flowchart for the RBMDO of cooling turbine blade, which contains four main steps:

### Step.1 Multidisciplinary analysis considering uncertainty

Uncertainties in material properties and working conditions need to be considered in the reliability-based multidisciplinary analysis of cooling turbine blade. Besides, in terms of geometry, the uncertainty focuses mainly on the blade profile, cooling structure and blade tenon for a typical cooling turbine

**Fig. 1** Illustration of the structure of cooling turbine blade (left) and its design matrix with fluid-thermal-solid interaction (right)



blade and a parameterized geometry model is essential to the following analyses.

### Step.2 Design of Experiment and Surrogate model initialization

Design of Experiment (DOE) is employed to obtain the Pareto graphs which show the effects of random and design variables on the responses. Moreover, design variables and responses obtained by DOE can be also used to initialize the surrogate model.

### Step.3 RBMDO loop

Following the initialized surrogate model, RBMDO of cooling turbine blade is conducted with a double loop approach, which integrates reliability analysis loop into the outer design optimization loop.

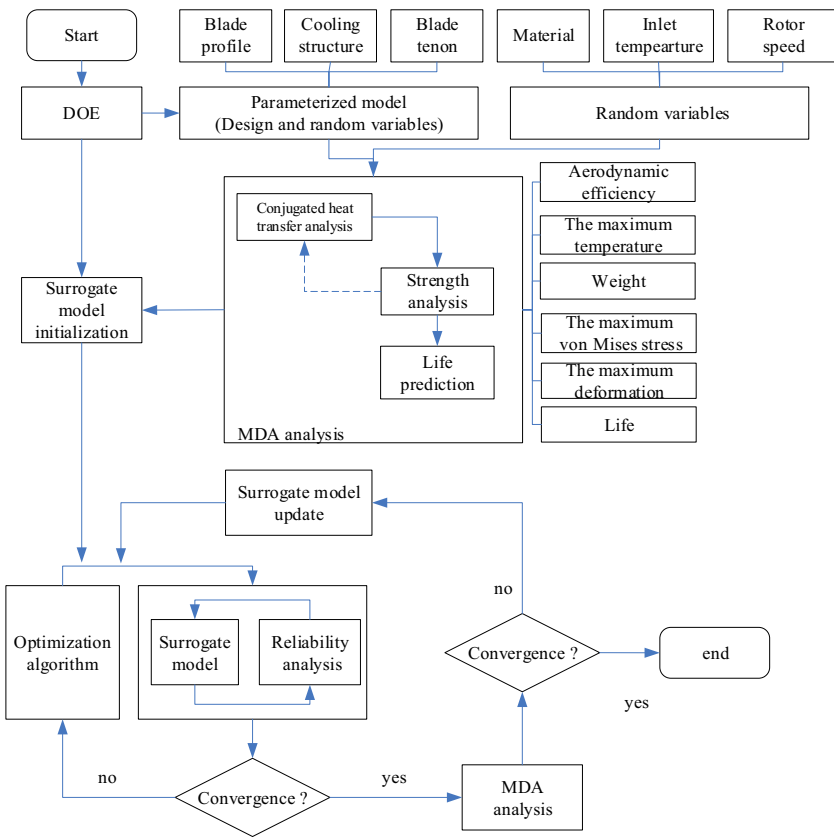
### Step.4 Updating Surrogate model

Surrogate model can save large amount of computing time, but it may not be as precise as the direct simulation of multidisciplinary analysis. If the optimized design point does not achieve the required precision, the surrogate model needs to be updated by adding new multidisciplinary analysis and the RBMDO loop will be repeatedly conducted until meeting the precision requirement.

## 3 Multidisciplinary analysis of a turbine cooling blade

Using the above methodology, a cooling turbine blade depicted in Fig. 3 is analyzed and optimized in this work. The shrouded blade has a predetermined section profile and variable wall thickness. Four ribs divide the hollow cooling turbine blade into five cooling passages, as shown in Fig. 3c. The cooling blade has three coolant inlets at the blade root and two outlets at the shroud and tailing edge. Pin-fin arrays with rectangular section are arranged near the tailing edge of the blade, as shown in Fig. 3d. The working rotor speed of blade is 9735 rpm.

**Fig. 2** RBMDO flowchart for cooling turbine blade



### 3.1 Conjugated heat transfer analysis

RNG-NS equations and SST  $k-\epsilon$  turbulence model, which have been validated by experimental data (Menter 1994; Wang et al. 2014; Garg and Ameri 2001), are employed to simulate the turbulent flow in both inner and outer domains of the example cooling turbine blade. Owing to circumferential periodicity, the model with only one blade and one flow passage is enough to capture the flow and heat transfer features of the cooling blade. Both outer and inner fluid domains are meshed by unstructured grids and boundary layer grid are refined in the near-wall regions. According to the reference (Song et al. 2017a, b), the thickness of the blade near-wall layer is about 5% of the blade chord length. The number of the boundary layer is 12 with the boundary layer height ratio of 1.2. As a result, the whole fluid domain is discretized into over 2 million grids and 350 thousand grid nodes. Using this mesh, the  $y^+$  calculated after analysis is less than 5 and most of  $y^+$  is less than 1. As for the structure domain, material of cooling turbine blade is K444 superalloy (Liu and Peng 2015) and its thermal properties are listed in Table 1. The structure domain is divided into over 1.56 million grids and 280 thousand grid nodes. Commercial CFD-Code ANSYS CFX which is widely used in heat transfer numerical predictions (Wang et al. 2018; Choi et al. 2017) is employed to analyze the conjugated heat transfer analysis of the turbine blade. Total pressure and static pressure conditions

are applied to the mainstream inlet and outlet respectively, interface between fluid analysis domain and solid analysis domain are set to be coupling surfaces. Figure 4 gives the obtained pressure distributions at three spanwise locations, i.e. 20%, 50 and 80% under 1.0 working condition that the rotating speed is 100% of the rated speed.

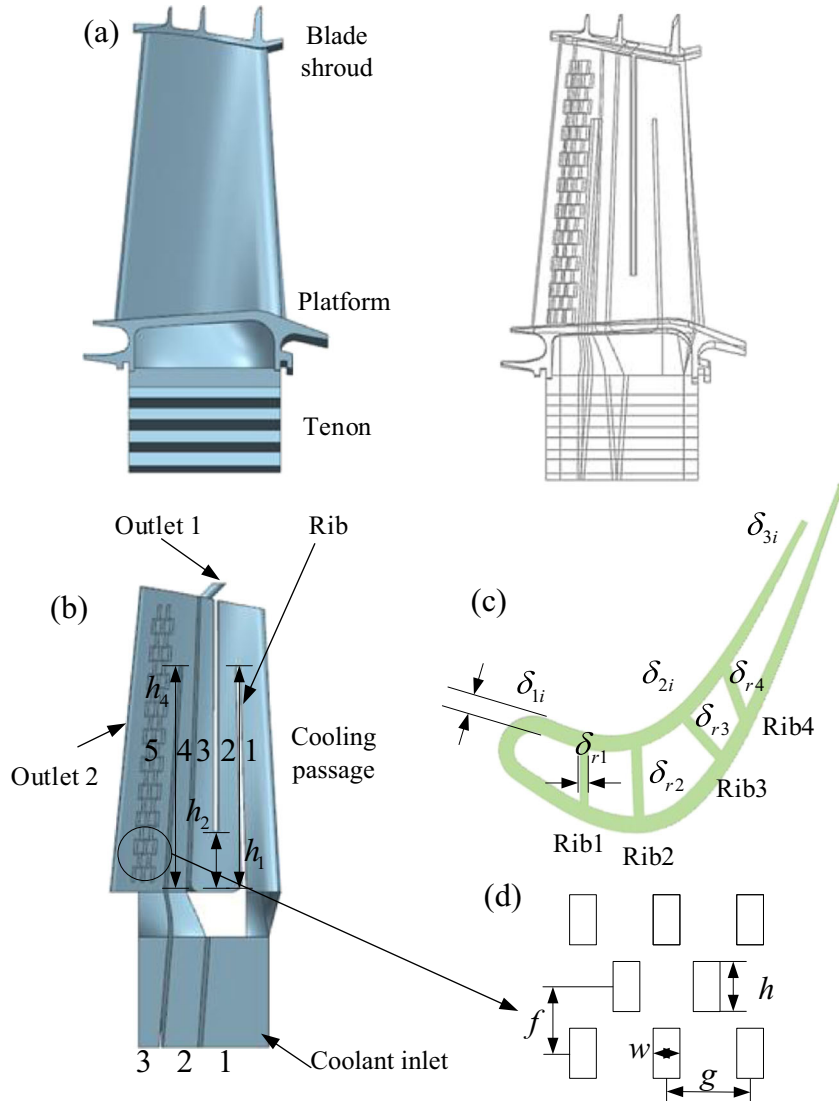
### 3.2 Temperature and pressure interpolation

The aerodynamic pressure on the coupling interfaces and temperature of cooling turbine blade obtained from the above analysis need to be interpolated to the structural analysis grid due to the mismatch between the interface grids for the heat transfer analysis and strength analysis. Here, the inverse distance-weighted average method (Zhang et al. 2016) is utilized to achieve the interpolation. Figure 5 shows good agreement between the temperature distribution on the blade pressure surface before and after interpolation, indicating the validity of our method.

### 3.3 Strength analysis

Finite element modeling (FEM) method is used to analyze the deformation and strength of the cooling turbine blade. The blade is fixed in the axial direction at the center point of its bottom; the contact constraint between turbine blade tenon

**Fig. 3** Geometry model of a cooling turbine blade, (a) turbine blade, (b) inner cooling structure, (c) cross section, (d) pin-fin arrays. Where,  $h_i (i = 1, 2, 4)$  represents the height of the ribs,  $\delta_{ri} (i = 1, \dots, 4)$  is the thickness of ribs, subscript  $i$  denotes the rib number from leading edge to tailing edge;  $\delta_{1i}, \delta_{2i}, \delta_{3i}$  represents the thickness of blade wall at different blade profile,  $j$  in this subscript denotes the blade profile at different blade height;  $h$  and  $w$  are the height and width of pin fin,  $g$  and  $f$  are the vertical and horizontal distance between pin fins



and turbine disc mortise is simplified into contact load on the contact surfaces. The magnitude of  $F$  is averaged from centrifugal load. Besides, there should be contact between adjacent blade shrouds in working condition. Therefore, three blades with contact constraints between middle blade and blade of both sides are modeled. Meanwhile, both two-side blades are fixed at their shrouds. Elasticity modulus  $E$ , Poisson's ratio  $\mu$ , shear modulus  $G$  and linear expansion coefficient  $\alpha$  of the K444 superalloy at different temperature listed in Table 2 are used for structural analysis in this work.

Figure 7 shows the von Mises stress distribution of the cooling turbine blade under 1.0 working condition. Because that

the stress in the blade tenon is not accurate due to the simplification of tenon contact loading, the stress above the blade tenon is only considered. As a consequence, the maximum stress is 783.24MPa, which is located in the rib at the blade root.

### 3.4 Life prediction

Two major damages, fatigue damage and creep damage, are considered in the life prediction of the analyzing blade under three working conditions, i.e. 1.0, 0.8 and 0.6. The working cycle compression spectrum and working time distribution spectrum are given in Fig. 8. Each working condition has its

**Table 1** Thermal properties of superalloy K444

Temperature /K	473	573	673	773	873	973	1073	1173	1273
Thermal conductivity [W/(m·°C)]	11.9	13.6	15.3	16.8	18.2	19.4	20.5	21.4	22.1
Specific heat capacity [J/(kg·°C)]	464	477	491	504	518	531	544	558	571

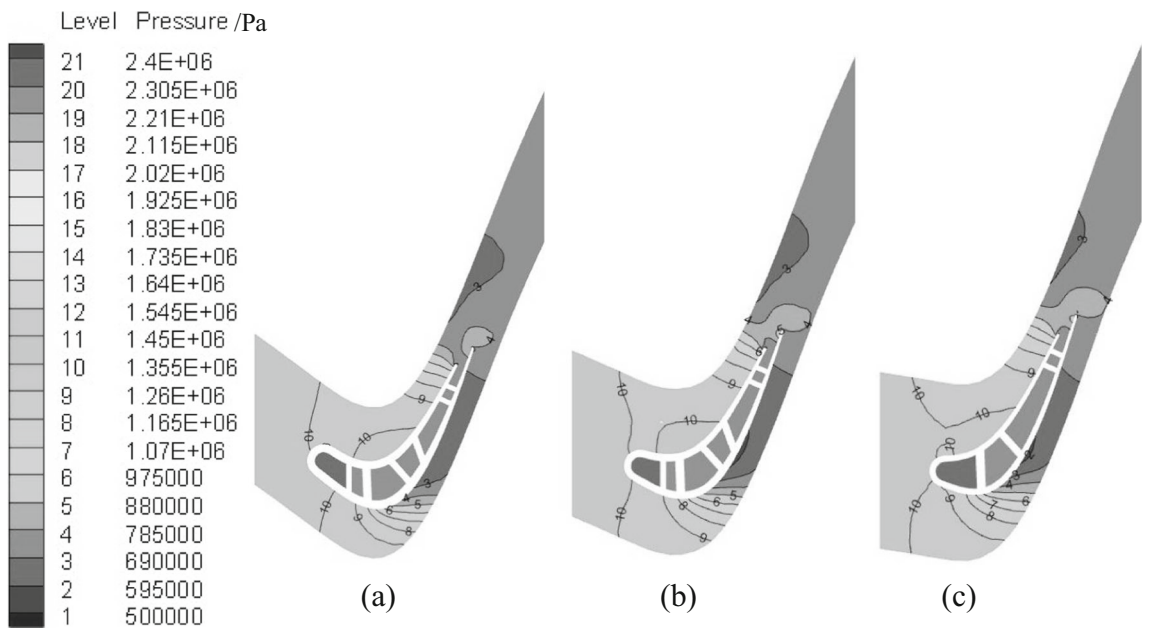


**Fig. 4** Pressure distributions on cross sections at different spanwise, (a) 20%, (b) 50%, (c) 80%

own rotation speed, inlet temperature, total inlet pressure, etc., so the fluid-thermal-solid interaction analysis needs to be carried out to obtain the temperature and stress of the blade under each working condition. After obtaining the stress and temperature of each working condition, the fatigue life is predicted by nominal stress method (Huang et al. 2017). Firstly, the stress amplitude and mean stress of cooling turbine blade in each working condition are converted to the stress amplitude with stress ratio  $R = -1$  by Goodman linear equation. Then, the fatigue cycle  $n$  under each working condition is calculated by SN curve of K444 superalloy. Creep life under each working condition is predicted by Larson Miller equation (Gupta and Haider 2014) which is stated as

$$\lg t_c = b_0 + b_1/T + b_2 \lg \sigma/T + b_3 (\lg \sigma)^2/T + b_4 (\lg \sigma)^3/T \quad (1)$$

Where,  $t_c$  is the creep life,  $T$  is the temperature,  $\sigma$  is the stress,  $b_i (i = 1, \dots, 4)$  is the material constant. Finally, the whole life of blade under three working conditions can be obtained by the Miner cumulative damage criteria (Chen and Ma 2012).

$$D = D_c + D_f \quad (2)$$

Where,  $D$  represents the whole damage of cooling turbine blade,  $D_c$  denotes the creep damage,  $D_f$  is the fatigue damage.

Fatigue and creep damages are intimately related to both stress and temperature of the cooling turbine blade. Since that the stress and temperature distributions are non-uniform, the

**Fig. 5** Comparison of temperature distribution on blade pressure surface between conjugated heat transfer analysis and that after interpolation, (a) conjugated heat transfer analysis, (b) interpolated

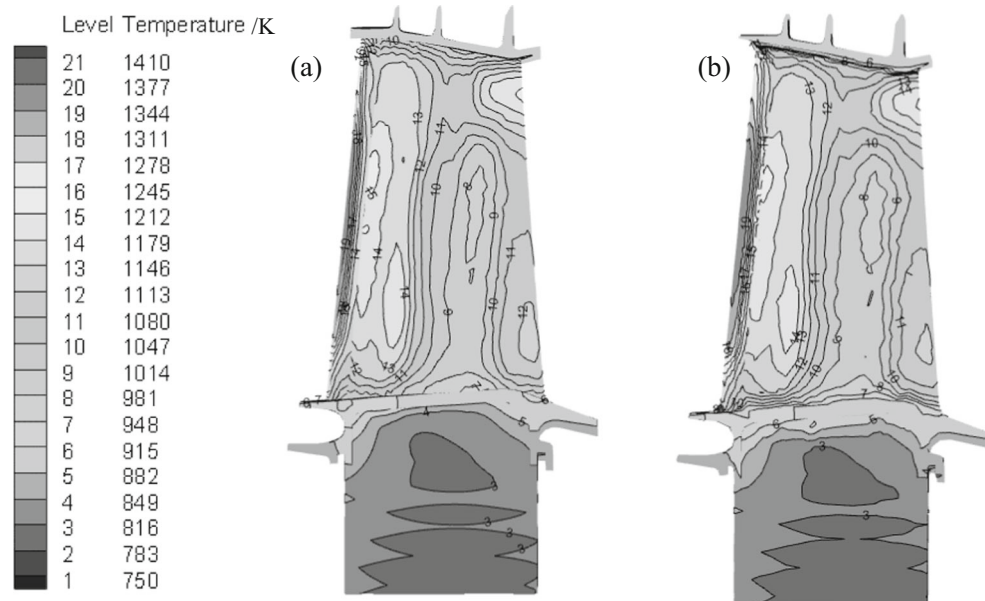
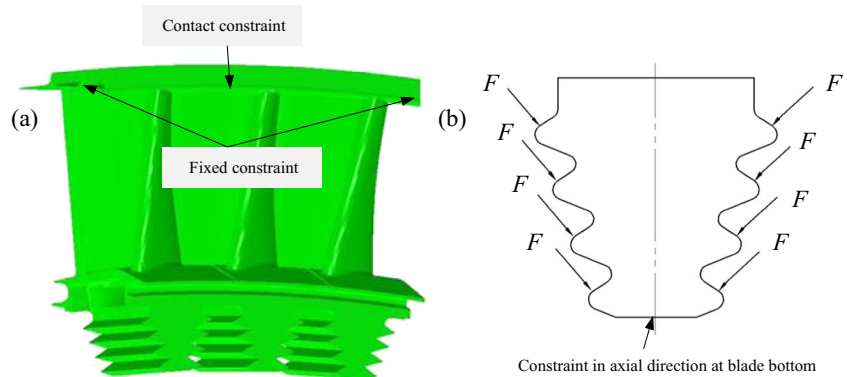


**Fig. 6** Constraint conditions of the cooling turbine blade, (a) contact constraints for platform and shroud, (b) constraints and loads applied to blade tenon



cooling turbine blade is divided into 8 partitions and the maximum damage is evaluated by considering the maximum stress region and the maximum temperature region in each blade partition. As a result, the crucial damage region is determined to be the maximum stress region in partition 2. The life of cooling turbine blade considering all the working conditions is 7922.675 h.

#### 4 Uncertainty data statistic and analysis

As mentioned above, the uncertainties of cooling turbine blade include geometry dimensions, material properties and working condition. In this section, the influences of main uncertainties on the cooling turbine blade are analyzed.

##### 4.1 Statistical probability models of uncertainties

The geometric uncertainties lie in the blade section profile, thickness of blade wall, thicknesses and heights of ribs, and the dimensions of shroud, blade root and pin-fin arrays. In this work, the uncertainty of blade profile will not be considered because that the dispersity of cast molding blade profile is small and has negligible effect on the performance of cooling turbine blade. Among all geometry uncertainties, the blade wall thickness, the thicknesses and heights of ribs have significant influences and are emphasized in the uncertainty analysis of this work.

Thickness data of cooling turbine blade is collected by measuring the real blades in which wall thickness is equal to rib thickness. The 150 thickness  $\delta$  of blade wall and rib on the

cross sections at different height of blade is measured, which is shown in Fig. 9. On basis of the measured data, the thickness difference  $\Delta\delta$  between the design data and measured data is calculated. All the thickness difference  $\Delta\delta$  is divided into 20 groups according to a constant thickness difference value and the probability density histogram shown in Fig. 9 is created. Statistical analysis of the collected data show that the thickness difference  $\Delta\delta$  obeys three-parameter Weibull distribution (by Kernel density estimation method (Yang and Yue 2014)) which is tested by the KS hypothesis with a significant level of 0.987. The three-parameter Weibull distribution is stated as

$$f(\Delta\delta) = \begin{cases} \frac{\beta}{\eta} \left( \frac{\Delta\delta - \alpha}{\eta} \right)^{(\beta-1)} e^{-\left(\frac{\Delta\delta - \alpha}{\eta}\right)^\beta} & \Delta\delta \geq \alpha \\ 0 & \Delta\delta < \alpha \end{cases} \quad (3)$$

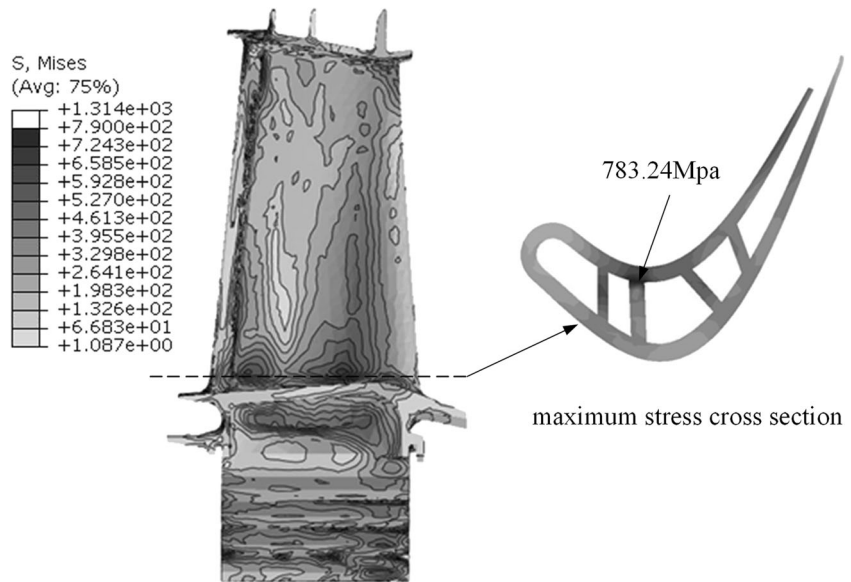
Where,  $\alpha$  is the location parameter,  $\beta$  is the shape parameter and  $\eta$  is the scale parameter, which are given in Fig. 9. Figure 9 plots the frequency histogram and three-parameter Weibull distribution curve.

The rotation speed  $r$  under 1.0 working condition of a turbine blade is collected, and more than 100 elastic modulus data are obtained. Using the similar process as thickness data analysis, the statistical analysis of the collected data is carried out. The results show that probability distributions of the elasticity Modulus  $E$  and rotation speed  $r$  also follow the three-parameter Weibull distribution, as shown in Fig. 10 and KS hypothesis tests indicate the significant levels of the Weibull distributions of  $E$  and  $r$  to be 0.8985 and 0.944, respectively. Therefore, the three-parameter Weibull distribution model can describe the uncertainties of  $\delta$ ,  $E$  and  $r$  with high precision.

**Table 2** Mechanical properties of superalloy K444

Temperature/K	293	373	473	573	673	773	873	973	1073	1173	1273
Elasticity modulus E/GPa	203	200	196	191	186	180	173	166	157	148	137
Shear modulus G/GPa	80	79	77	75	72	70	67	64	60	56	52
Poisson's ratio $\mu$	0.27	0.27	0.27	0.27	0.29	0.29	0.29	0.30	0.31	0.32	0.32
Linear expansion coefficient $\alpha$ ( $10^{-6}$ $^{\circ}\text{C}^{-1}$ )	–	12.0	12.4	12.6	12.9	13.2	13.5	13.9	14.4	14.9	15.5

**Fig. 7** The von Mises stress distribution of cooling turbine blade



#### 4.2 Influences of uncertainties on performance of cooling turbine blade

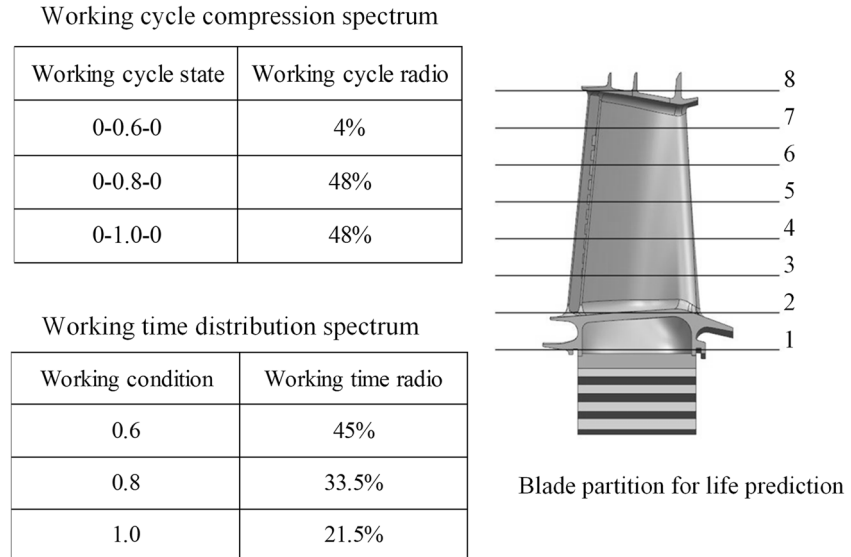
Here, the effects of uncertainties on the heat transfer, strength and life of the cooling turbine blade are analyzed. Table 3 lists the uncertain factors considered in the present work, in which  $\delta_{1i}$ ,  $\delta_{2i}$ ,  $\delta_{3i}$  denotes the thickness of cooling blade wall, where subscript 1, 2, 3 represents the position in the blade cross section and subscript  $i = 1, 2$  represents the cross section at blade root and tip. Besides,  $\delta_{ri}(i=1, \dots, 4)$  and  $h_i(i=1, \dots, 4)$  are the thicknesses and heights of the ribs, respectively, where subscript  $i = 1, \dots, 4$  denotes the rib number from leading edge to tailing edge, as shown in Fig. 3. Due to the lack of statistical data, the heights of ribs  $h_i(i=1, \dots, 4)$  and the Poisson ratio of K444 material are assumed to follow normal distribution. And assume that all random variables are independent of each other.

The influences of random variables on multidisciplinary characteristics of the original cooling turbine blade under 1.0 working condition is analyzed. Figure 11 indicates that the dispersivity in the average temperature, the highest temperature, the maximum von Mises stress and damage can be significantly large under random variables. For example, the maximum difference of the highest temperature under random variables reaches 190.8 K, which is about 19% of the average value.

#### 5 Optimization and results

The main goal of designing cooling turbine blade is to achieve long working time. Because that the blade life is related to the temperature and stress, the minimum average temperature and the maximum damage of the cooling turbine blade are chosen

**Fig. 8** Life prediction of cooling turbine blade



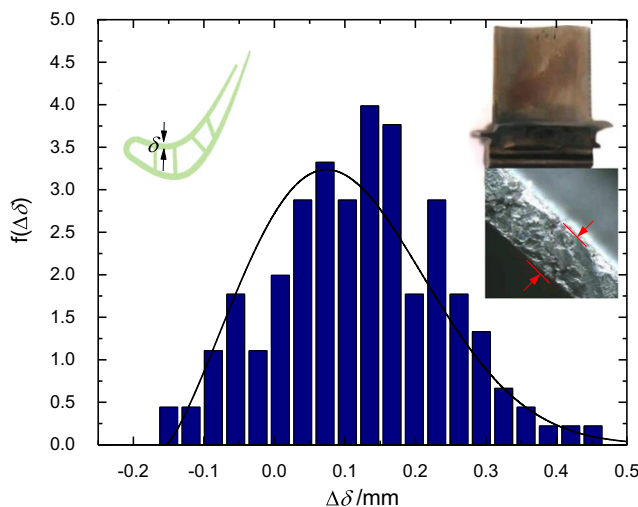
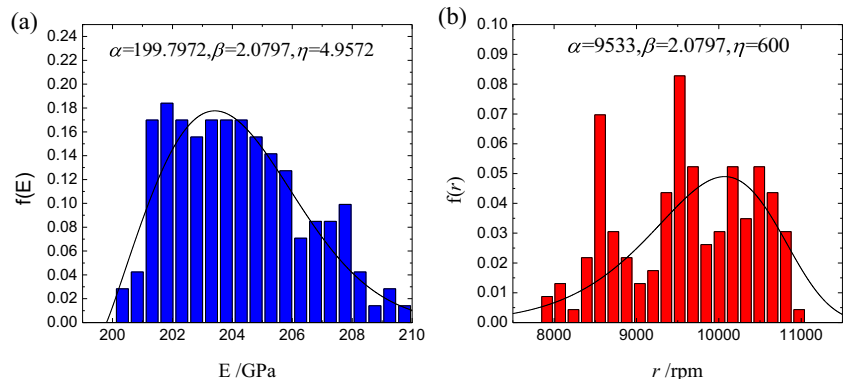


**Fig. 9** Frequency histogram and 3 parameters Weibull distribution curve of thickness,  $\alpha = -0.1540$ ,  $\beta = 2.2979$ ,  $\eta = 0.2923$

as the optimization objectives. Besides, the highest temperature and the maximum von Mises stress should be less than the allowable values during optimization, which are chosen as the constrain conditions in the optimization. The reliabilities of the blade life is also constraint conditions. Because that the characteristics of cooling turbine blade working at 0.8 and 0.6 conditions are similar to the characteristic of 1.0 condition. In order to simplify optimization process, only cooling turbine blade under 1.0 working condition is analyzed in RBMDO cycle. The objective of longest blade working life is converted to the minimal damage under 1.0 working condition. The RBMDO problem of the cooling turbine blade can be formulated as

$$\left\{ \begin{array}{l} \text{find } \mathbf{x} \\ \min f = w_1 \cdot D(\mathbf{x}, \mathbf{y}) + w_2 \cdot T_{ave}(\mathbf{x}, \mathbf{y}) \\ \text{s.t. } T_{max}(\mathbf{x}, \mathbf{y}) \leq [1500K] \\ \sigma_{max}(\mathbf{x}, \mathbf{y}) \leq [830Mpa] \\ P\{D(\mathbf{x}, \mathbf{y}) - [0.32] \geq 0\} \geq 99.9\% \\ \mathbf{x}^l \leq \mathbf{x} \leq \mathbf{x}^u \\ \mathbf{y} \in \text{weibull or normal} \end{array} \right. \quad (4)$$

**Fig. 10** Probability distribution of elasticity Modulus  $E$  and rotation speed  $r$ , (a) and (b) three-parameter Weibull distribution curve of  $E$  and  $r$



where,  $f$  is the objective function,  $D(\mathbf{x}, \mathbf{y})$  is the damage of cooling turbine blade,  $T_{ave}(\mathbf{x}, \mathbf{y})$  denotes the average temperature,  $w_1 = 3000$  and  $w_2 = 1$  are the weight factor;  $T_{max}(\mathbf{x}, \mathbf{y})$  is the maximum temperature of cooling turbine blade.  $\sigma_{max}(\mathbf{x}, \mathbf{y})$  is the maximum stress.  $P$  represents the reliability.  $\mathbf{x}$  is the design variable vector including rib height  $h_i$ , ribs thickness  $\delta_{ri}$ , blade thickness  $\delta_{1i}$ , design parameters of pin fins and is well described in Fig. 1, the superscripts  $L$  and  $U$  represent the lower limit and upper limit;  $\mathbf{y}$  is the vector of random variables which is listed in Table 3.

### 5.1 DOE and surrogate model of cooling turbine blade

DOE of cooling turbine blade is carried out by optimal Latin hypercube method (Stocki 2005) to obtain the initial data of cooling turbine blade in this paper. The lower and upper limit of the variables are given in Table 4. In total, 20 factors and 100 level experiments are obtained by conducting multidisciplinary analysis of the cooling turbine blade.

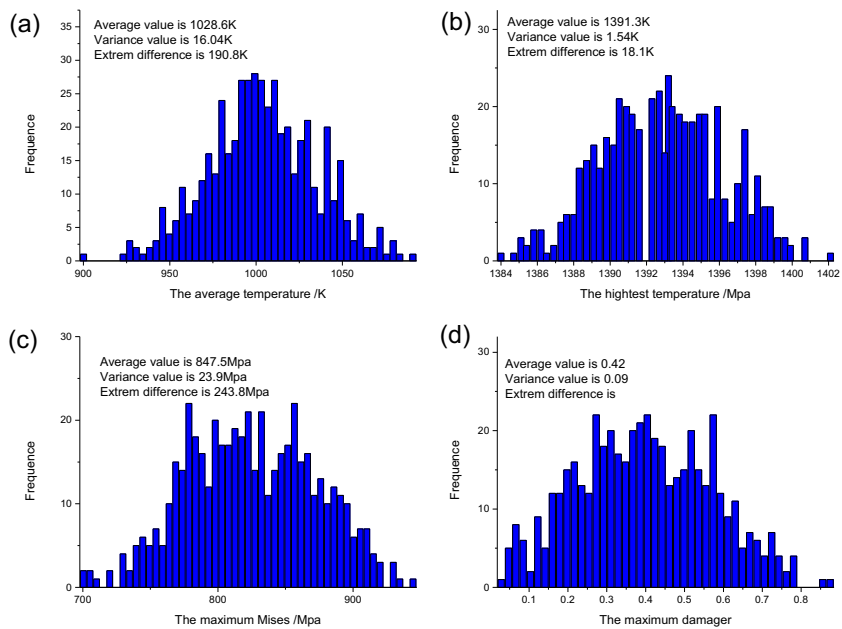
Then, the Kriging surrogate model for replacing the multidisciplinary analysis in the RBMDO is initialized based on the sampling data points from DOE. Figure 12 gives Kriging fitting surfaces of the cooling turbine blade performance (life, the maximum von Mises stress, the maximum temperature and average temperature) with respect to  $\delta_{r4}$  and  $\delta_{11}$ , when other variables are set to be constant. Root mean square errors of the Kriging models are all less than 0.01 and meet the precision requirements of the optimization.

### 5.2 Results and discussion

Reliability of cooling turbine blade is analyzed by advanced first order second moment method. To avoid falling into the local optimal solution, Multi-island genetic algorithm and nonlinear Sequential Quadratic Programming algorithm are combined to optimize the RBMDO of cooling turbine blade sequentially.

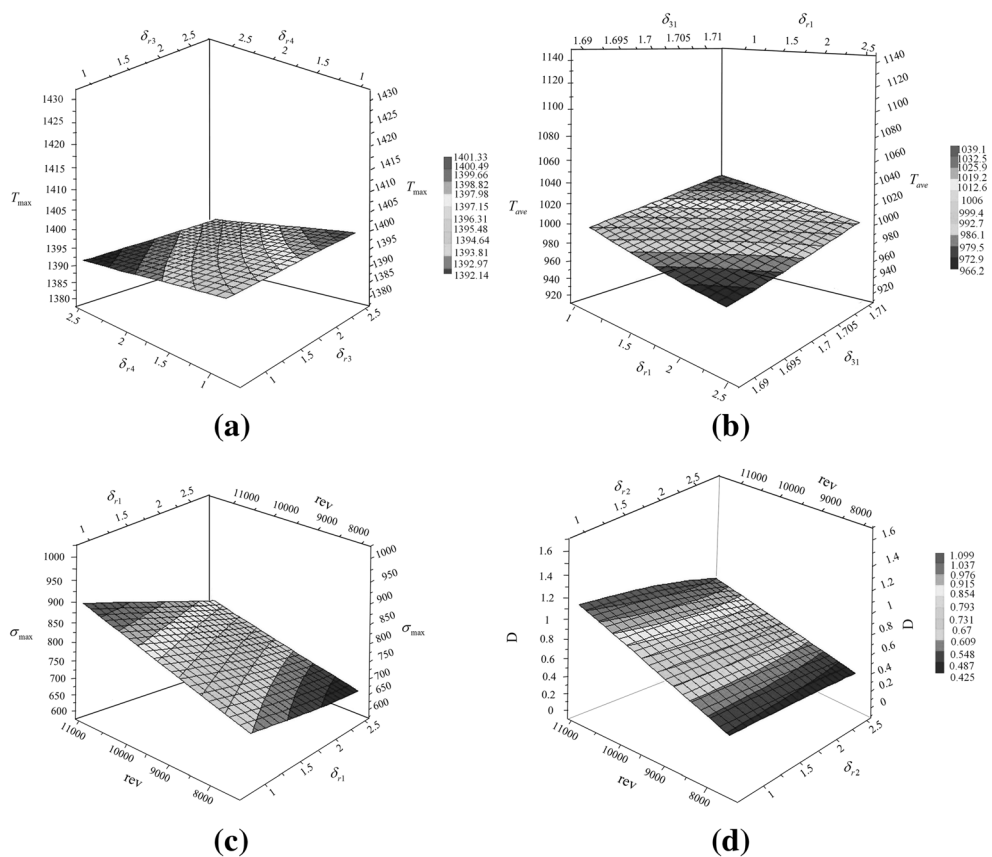
**Table 3** Random variables and distribution form

Random variables		Distribution form
Category	Variables	
Geometry size	$\delta_{11}, \delta_{21}, \delta_{31}, \delta_{12}, \delta_{22}, \delta_{32}$	three-parameter Weibull distribution
	$\delta_{r1}, \delta_{r2}, \delta_{r3}, \delta_{r4}$	three-parameter Weibull distribution
	$h_1, h_2, h_4$	Normal distribution
Material mechanical properties	Elasticity Modulus	three-parameter Weibull distribution
	Poisson ratio	Normal distribution
Working condition	Rotation speed	three-parameter Weibull distribution

**Fig. 11** Frequency histogram for (a) average temperature, (b) the highest temperature, (c) the maximum von Mises stress, (d) the maximum damage under 1.0 working condition**Table 4** The lower and upper limit of variables of DOE

Variables		Lower limit	Upper limit
height of the rib 1	$h_1/\text{mm}$	40.0	44.0
thickness of rib 1	$\delta_{r1}/\text{mm}$	1.0	2.0
height of the rib 2	$h_2/\text{mm}$	5.0	10.0
thickness of rib 2	$\delta_{r2}/\text{mm}$	1.0	2.0
thickness of rib 3	$\delta_{r3}/\text{mm}$	1.0	2.0
height of the rib 4	$h_4/\text{mm}$	40.0	44.0
thickness of rib 4	$\delta_{r4}/\text{mm}$	1.0	2.0
blade wall thickness at root of blade cross section	$\delta_{11}/\text{mm}$ $\delta_{21}/\text{mm}$ $\delta_{31}/\text{mm}$	1.69 1.69 1.69	1.71 1.71 1.71
blade wall thickness at top of blade cross section	$\delta_{12}/\text{mm}$ $\delta_{22}/\text{mm}$ $\delta_{32}/\text{mm}$	1.2 1.2 1.0	1.25 1.25 1.05
height of pin fin	$h/\text{mm}$	2.2	2.7
width of pin fin	$w/\text{mm}$	1.0	1.5
vertical distance between pin fins	$g/\text{mm}$	4.0	4.8
horizontal distance between pin fins	$f/\text{mm}$	3.2	4.8
Rotator speed /rpm		7300	12,000
Elasticity modulus /Mpa		E-10%	E + 10%
Poisson ratio		$\mu-10\%$	$\mu + 10\%$

**Fig. 12** Kriging fitting surface of cooling turbine blade along  $\delta_{r4}$  and  $\delta_{11}$ , (a) average temperature, (b) the maximum temperature, (c) the maximum von Mises stress, (d) life damage



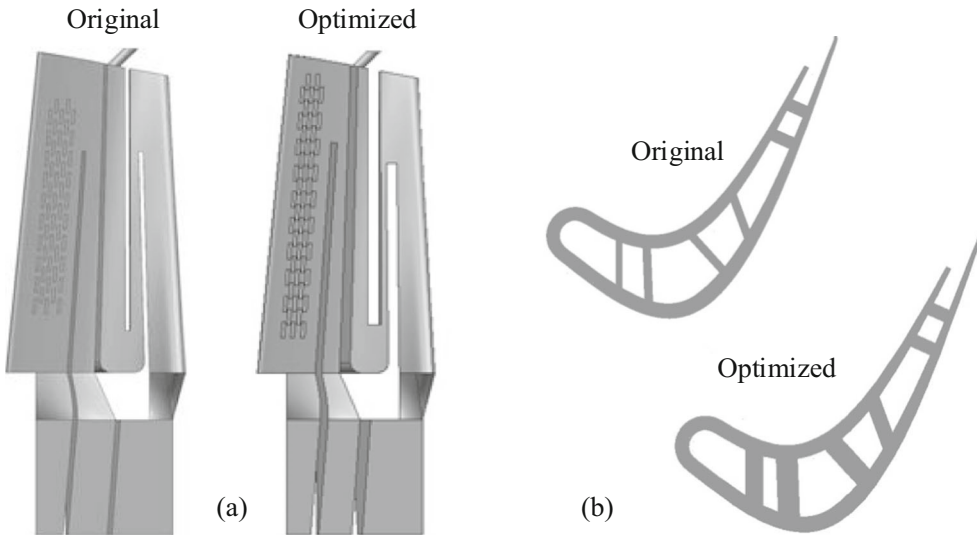
According to the number of the design variables and the MDA results of the cooling turbine blade reflected from DOE data, the populations, islands and generations of multi-island genetic algorithm are set to 10. Then, taking the optimal design variables of multi-island genetic algorithm as the initial value, the optimization is driven by nonlinear Sequential Quadratic Programming algo-

rithm with the convergence of  $10^{-6}$ . Meanwhile, the deterministic MDO is also carried out on basis of the process of RBMDO. Table 5 gives the values of design variables, which include the original value, the optimized value of deterministic MDO and the optimized value of RBMDO. Figure 13 gives the comparison of the cooling structure of turbine blade before and after

**Table 5** Comparison of design variables before and after optimization

Design variables	Original /mm		Optimized /mm	
	MDO	RBMDO	MDO	RBMDO
height of the rib 1	$h_1$	42.0	44.5	40.127
thickness of rib 1	$\delta_{r1}$	1.0	2.5	2.4633
height of the rib 2	$h_2$	8.0	10.5	9.2574
thickness of rib 2	$\delta_{r2}$	1.0	2.0138	2.4316
thickness of rib 3	$\delta_{r3}$	1.0	2.4275	2.2403
height of the rib 4	$h_4$	42.0	44.456	44.08
thickness of rib 4	$\delta_{r4}$	1.0	2.4975	1.6709
blade wall thickness at root of blade cross section	$\delta_{11}$	1.70	1.7	1.7073
blade wall thickness at top of blade cross section	$\delta_{21}$	1.69	1.709	1.6939
	$\delta_{31}$	1.69	1.6917	1.7068
height of pin fin	$\delta_{12}$	1.2	1.23	1.2276
width of pin fin	$\delta_{22}$	1.2	1.2	1.2023
vertical distance between pin fins	$\delta_{32}$	1.0	1.05	1.0464
horizontal distance between pin fins	$h$	2.5	2.41	2.41
	$w$	1.0	1.14	1.14
	$g$	4.0	4.49	4.49
	$f$	4.8	4.12	4.12

**Fig. 13** Comparison of cooling structure before and after optimization, (a) entire cooling structure, (b) blade cross section at 50% spanwise



optimization by RBMDO. From the result, it can be seen that the thickness of cooling turbine blade wall and ribs after optimization increase obviously comparing with the original. After optimization of RBMDO, the rib height  $h_1$ ,  $h_2$  and  $h_4$  also change and cause the five cooling passages of turbine blade to change. Table 6 gives comparison of objectives and constraints before and after optimization, indicating that the average temperature and damage are reduced by 12.28 and 23.45% after optimization respectively. The overall blade life under all working condition after optimization of RBMDO is 9411.7 h.

The temperature distribution under 1.0 working condition before and after optimization of RBMDO is compared in Fig. 14. It can be seen that area of the high temperature regions of optimized blade are obviously reduced contrary to the original blade, which are labeled with A and B. The temperature on region A is mainly affected by the cooling passage 1, 2 and 3; The temperature on region B is mainly affected by the cooling passage 4 and 5. The cross section area of cooling passage 2 and 3 after optimization reduce so that the flow velocity of

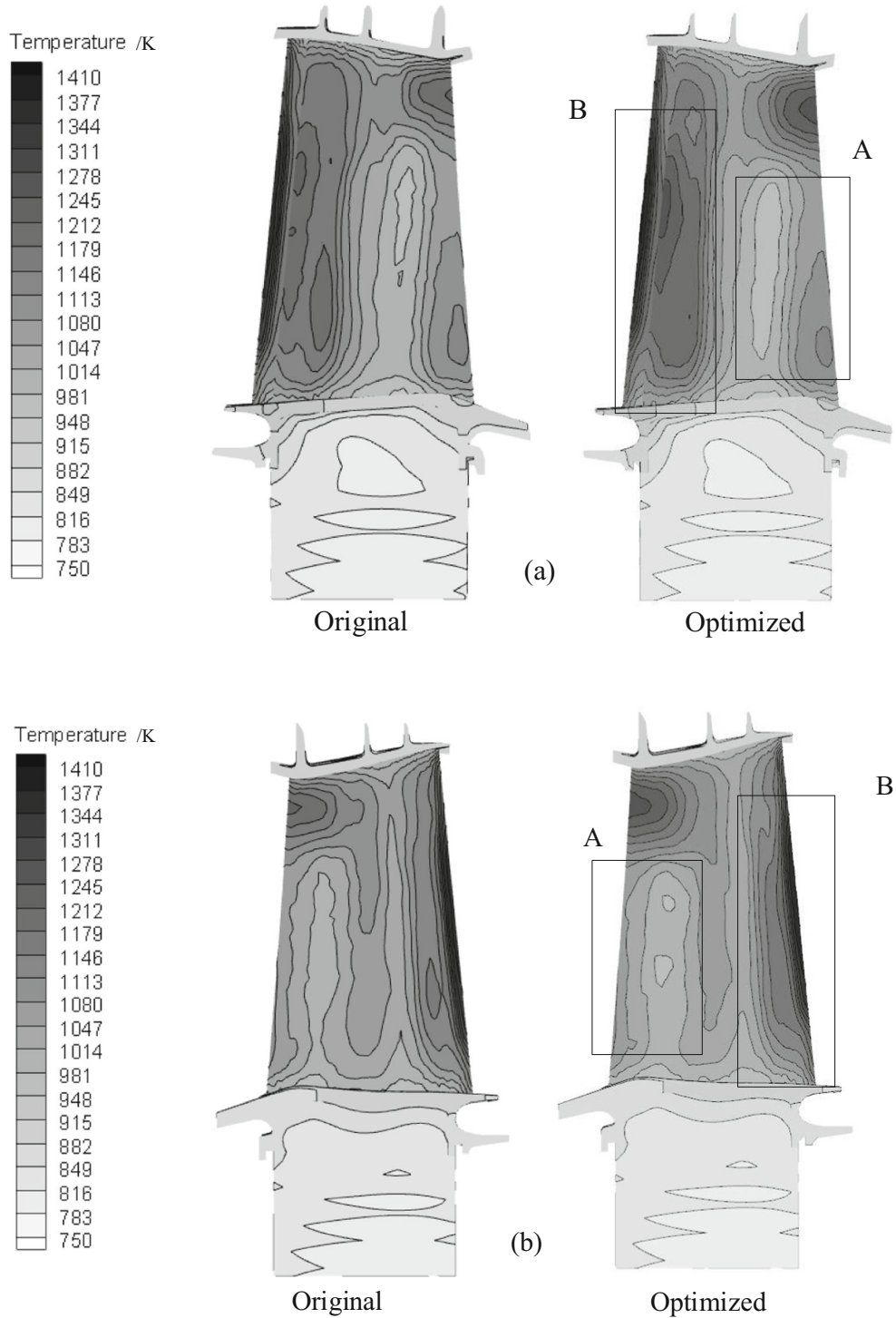
coolant will raise to enhance the local convective heat transfer. In the region B, the cross section area of cooling passage 4 reduces to increase the flow velocity of coolant, and the pin fins in the cooling passage 5 after optimization cause more coolant flow out near the top to reduce the temperature of this region.

The von Mises stress distribution under 1.0 working condition before and after optimization of RBMDO is compared in Fig. 15. It can be seen that higher stress region at root, leading edge and tailing edge of the cooling turbine blade is significantly reduced, which are labeled with A and B in Fig. 15. The stress of cooling blade is directly related to the centrifugal load and temperature load. From the result of the Fig. 14 shows, the temperature gradient in the region A and B of Fig. 15 decreases to reduce the temperature stress. In the state of rotation, the thickness of blade wall and ribs increasing may increase stress causing by centrifugal load or may reduce stress causing by centrifugal load. Overall, the reducing of blade temperature and the increasing of blade wall and ribs thickness cause that the Maximum stress reduce and life increase.

**Table 6** Comparison of objectives and constraints before and after optimization

	Objectives or constraints	Original	Optimized		Relative variation
		MDO	RBMDO		
$T_{ave} /K$	↓	1103.59	934.78	968.05	12.28%
$D$	↓	0.307	0.256	0.235	23.45%
$\sigma_{max} /MPa$	<830	783.24	776.43	779.8	
$T_{max} /K$	<1500	1393.26	1398.4	1390.3	
Life reliability	>99.9%	0.997	—	0.999	
Life /h		7922.675		9411.7	

**Fig. 14** Comparison of temperature distribution before and after optimization, (a) pressure surface side, (b) suction surface side

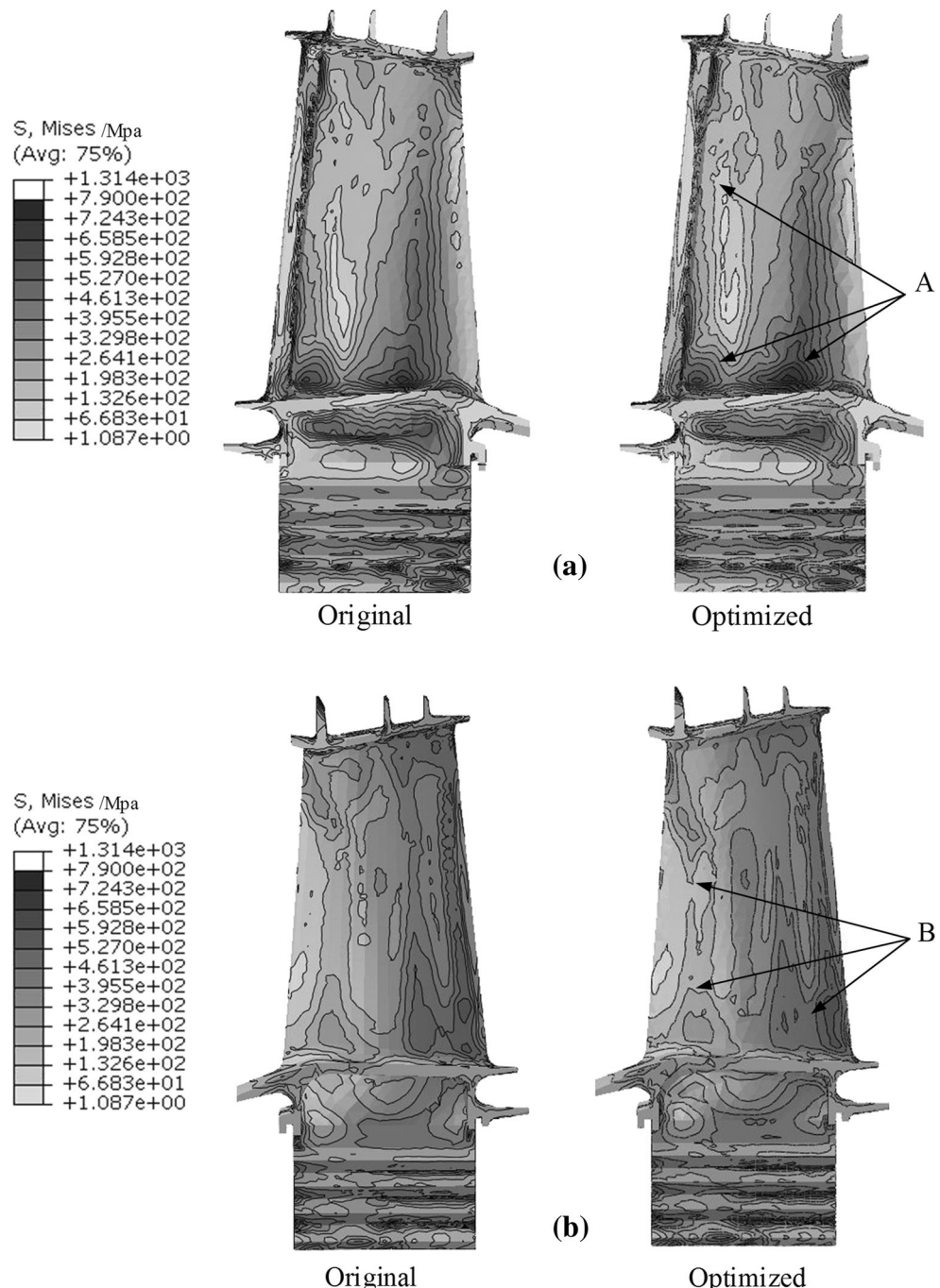


## 6 Concluding remarks

Because of the complex manufacturing process and terrible working conditions, the cooling turbine blade has become more prone to failure. Uncertainties of cooling turbine blade include geometry dimensions, material properties and working condition. Statistical analysis of the collected data show that probability

distributions of blade wall thickness, elasticity Modulus and rotation speed follow the three-parameter Weibull distribution. The influence of random variables on multidisciplinary characteristics of the original cooling turbine blade under 1.0 working condition is analyzed. Results show that uncertainties considered in this work have an evident influence on the temperature and stress of the blade.

**Fig. 15** Comparison of von Mises stress distribution before and after optimization, (a) pressure surface side, (b) suction surface side



Considering the coupling among aerodynamic, heat transfer and strength, a RBMDO method for cooling turbine blade on basis of MDA framework adding reliability analysis loop is introduced, which contains four main steps: multidisciplinary analysis considering uncertainties, Design of Experiment and surrogate model initialization, RBMDO loop and surrogate model Updating. Sequential conjugated heat transfer analysis and strength analysis with temperature and pressure interpolation is used to obtain multidisciplinary coupling analysis of

cooling turbine blade. Surrogate model is introduced to reduce time-consuming multidisciplinary reliability analysis in RBMDO loop. Optimization results shows that the RBMDO method proposed in this work improves the performance of cooling turbine blade available.

**Acknowledgments** National Natural Science Foundation of China (Grant No. 51575444), Aerospace Science and Technology Foundation (Grant No. 2017-HT-XGD), Aviation Power Foundation (Grant No. 6141B090319) support this work.

**Publisher's Note** Springer Nature remains neutral with regard to jurisdictional claims in published maps and institutional affiliations.

## References

- Ahn J, Kwon JH (2006) An efficient strategy for reliability-based multidisciplinary design optimization using BLISS. *Struct Multidiscip Optim* 31(5):363–372
- Bejan A (2013) Convection heat transfer. Wiley, Hoboken
- Chen QF, Ma XB (2012) Research of aircraft SHP method based on changed loading spectrum. Prognostics and system health management (PHM), 2012 IEEE conference on. IEEE 2012: 1–5
- Chen ZZ, Qiu HB, Gao L, Li XK, Li PG (2014) A local adaptive sampling method for reliability-based design optimization using kriging model. *Struct Multidiscip Optim* 49(3):401–416
- Choi SM, Park JS, Chung H, Park S, Cho HH (2017) Upstream wake effect on flow and heat transfer characteristics at an endwall of first-stage blade of a gas turbine. *Exp Thermal Fluid Sci* 86:23–36
- Deng S, Suresh K (2017a) Stress constrained thermo-elastic topology optimization with varying temperature fields via augmented topological sensitivity based level-set. *Struct Multidiscip Optim* 56(6):1413–1427
- Deng S, Suresh K (2017b) Topology optimization under thermo-elastic buckling. *Struct Multidiscip Optim* 55(5):1759–1772
- Du X, Guo J, Beoram H (2008) Sequential optimization and reliability assessment for multidisciplinary systems design. *Struct Multidiscip Optim* 35(2):117–130
- Fei C, Bai G (2012) Extremum selection method of random variable for nonlinear dynamic reliability analysis of turbine blade deformation. *Propulsion and Power Research* 1(1):58–63
- Gao HF, Fei CW, Bai GC, Ding L (2016) Reliability-based low-cycle fatigue damage analysis for turbine blade with thermo-structural interaction. *Aerospace Science and Technology* 49: 289–300
- Garg VK, Ameri AA (2001) Two-equation turbulence models for prediction of heat transfer on a transonic turbine blade. *Int J Heat Fluid Flow* 22(6):593–602
- Gupta AK, Haider MR (2014) Creep Life Estimation of Low Pressure Reaction Turbine Blade. *International Journal of Technological Exploration and Learning (IJTEL)* 3(2):402–404
- Huang HZ, Huang CG, Peng Z, Li YF, Yin H (2017) Fatigue life prediction of fan blade using nominal stress method and cumulative fatigue damage theory. *International Journal of Turbo & Jet-Engines*. <https://doi.org/10.1515/ijtj-2017-0015>
- Huang ZL, Zhou YS, Jiang C, Zheng L, Han X (2018) Reliability-based multidisciplinary design optimization using incremental shifting vector strategy and its application in electronic product design. *Acta Mech Sinica* 34(2):285–302
- Hui F, Weiji L (2008) An efficient method for reliability-based multidisciplinary design optimization. *Chin J Aeronaut* 21(4):335–340
- Li XK, Qiu HB, Chen ZZ, Gao L, Shao XY (2016) A local kriging approximation method using MPP for reliability-based design optimization. *Comput Struct* 162:102–115
- Liu CJ, Peng JQ (2015) Four hot corrosion resistant materials for IGT blades. *Procedia Engineering* 130:662–667
- Meng D, Li YF, Huang HZ, Zhang X, Liu Y (2015) Reliability-based multidisciplinary design optimization using subset simulation analysis and its application in the hydraulic transmission mechanism design. *J Mech Des* 137(5):051402
- Menter FR (1994) Two-equation eddy-viscosity turbulence models for engineering applications. *AIAA J* 32(8):1598–1605
- Nikbay M, Kuru MN (2013) Reliability based multidisciplinary optimization of aeroelastic systems with structural and aerodynamic uncertainties. *J Aircr* 50(3):708–715
- Park HW, Kim MS, Choi DH, Mavris DN (2002) Optimizing the Parallel Process Flow for the Individual Discipline Feasible Method. 9th AIAA/ISSMO Symposium on Multidisciplinary Analysis and Optimization: 5411
- Perez R, Liu H, Behdinan K (2004) Evaluation of multidisciplinary optimization approaches for aircraft conceptual design. 10th AIAA/ISSMO multidisciplinary analysis and optimization conference: 4537
- Roshanian J, Ebrahimi M (2013) Latin hypercube sampling applied to reliability-based multidisciplinary design optimization of a launch vehicle. *Aerosp Sci Technol* 28(1):297–304
- Saad L, Aissani A, Chateauneuf A, Raphael W (2016) Reliability-based optimization of direct and indirect LCC of RC bridge elements under coupled fatigue-corrosion deterioration processes. *Eng Fail Anal* 59:570–587
- Sellar R, Batill S, Renaud J (1996) Response surface based, concurrent subspace optimization for multidisciplinary system design. 34th Aerospace Sciences Meeting and Exhibit: 714
- Song LK, Fei CW, Wen J, Bai GC (2017a) Multi-objective reliability-based design optimization approach of complex structure with multi-failure modes. *Aerosp Sci Technol* 64:52–62
- Song L, Zhu P, Li J, Feng Z (2017b) Effect of purge flow on endwall flow and heat transfer characteristics of a gas turbine blade. *Appl Therm Eng* 110:504–520
- Stocki R (2005) A method to improve design reliability using optimal Latin hypercube sampling. *Comput Assist Mech Eng Sci* 12(4):393
- Wang L, Wang S, Wen F, Zhou X, Wang Z (2018) Effects of continuous wavy ribs on heat transfer and cooling air flow in a square single-pass channel of turbine blade. *Int J Heat Mass Transf* 121:514–533
- Wang P, Li Y, Zou Z, Wang L, Song S (2014) Influence of turbulence model parameter settings on conjugate heat transfer simulation. *Heat Mass Transf* 50(4):521–532
- Wang XH, Li RJ, Xia RW (2013) Comparison of MDO methods for an Earth observation satellite. *Procedia Engineering* 67:166–177
- Wong CN, Huang HZ, Li N (2013) Fourier series based reliability analysis of aeroengine turbine blade under linear fuzzy safety state. *Eng Fail Anal* 31:268–280
- Yang F, Yue Z (2014) Kernel density estimation of three-parameter Weibull distribution with neural network and genetic algorithm. *Appl Math Comput* 247:803–814
- Yao W, Chen X, Luo W, Tooren MV, Guo J (2011) Review of uncertainty-based multidisciplinary design optimization methods for aerospace vehicles. *Prog Aerosp Sci* 47(6):450–479
- Zhang MC, Gou WX, Li L, Wang XM, Yue ZF (2016) Multidisciplinary design and optimization of the twin-web turbine disk. *Struct Multidiscip Optim* 53(5):1129–1141
- Zhou H, Jiang P, Shao X, Yi Y (2014) An improved bi-level integrated system collaborative optimization method for multidisciplinary design optimization. *Modelling, Identification & Control (ICMIC)*, 2014 Proceedings of the 6th International Conference on IEEE: 365–370

## Terms and Conditions

Springer Nature journal content, brought to you courtesy of Springer Nature Customer Service Center GmbH (“Springer Nature”). Springer Nature supports a reasonable amount of sharing of research papers by authors, subscribers and authorised users (“Users”), for small-scale personal, non-commercial use provided that all copyright, trade and service marks and other proprietary notices are maintained. By accessing, sharing, receiving or otherwise using the Springer Nature journal content you agree to these terms of use (“Terms”). For these purposes, Springer Nature considers academic use (by researchers and students) to be non-commercial.

These Terms are supplementary and will apply in addition to any applicable website terms and conditions, a relevant site licence or a personal subscription. These Terms will prevail over any conflict or ambiguity with regards to the relevant terms, a site licence or a personal subscription (to the extent of the conflict or ambiguity only). For Creative Commons-licensed articles, the terms of the Creative Commons license used will apply.

We collect and use personal data to provide access to the Springer Nature journal content. We may also use these personal data internally within ResearchGate and Springer Nature and as agreed share it, in an anonymised way, for purposes of tracking, analysis and reporting. We will not otherwise disclose your personal data outside the ResearchGate or the Springer Nature group of companies unless we have your permission as detailed in the Privacy Policy.

While Users may use the Springer Nature journal content for small scale, personal non-commercial use, it is important to note that Users may not:

1. use such content for the purpose of providing other users with access on a regular or large scale basis or as a means to circumvent access control;
2. use such content where to do so would be considered a criminal or statutory offence in any jurisdiction, or gives rise to civil liability, or is otherwise unlawful;
3. falsely or misleadingly imply or suggest endorsement, approval , sponsorship, or association unless explicitly agreed to by Springer Nature in writing;
4. use bots or other automated methods to access the content or redirect messages
5. override any security feature or exclusionary protocol; or
6. share the content in order to create substitute for Springer Nature products or services or a systematic database of Springer Nature journal content.

In line with the restriction against commercial use, Springer Nature does not permit the creation of a product or service that creates revenue, royalties, rent or income from our content or its inclusion as part of a paid for service or for other commercial gain. Springer Nature journal content cannot be used for inter-library loans and librarians may not upload Springer Nature journal content on a large scale into their, or any other, institutional repository.

These terms of use are reviewed regularly and may be amended at any time. Springer Nature is not obligated to publish any information or content on this website and may remove it or features or functionality at our sole discretion, at any time with or without notice. Springer Nature may revoke this licence to you at any time and remove access to any copies of the Springer Nature journal content which have been saved.

To the fullest extent permitted by law, Springer Nature makes no warranties, representations or guarantees to Users, either express or implied with respect to the Springer nature journal content and all parties disclaim and waive any implied warranties or warranties imposed by law, including merchantability or fitness for any particular purpose.

Please note that these rights do not automatically extend to content, data or other material published by Springer Nature that may be licensed from third parties.

If you would like to use or distribute our Springer Nature journal content to a wider audience or on a regular basis or in any other manner not expressly permitted by these Terms, please contact Springer Nature at

[onlineservice@springernature.com](mailto:onlineservice@springernature.com)